Modeling Leakage Kinetics from Multilamellar Vesicles for Membrane Permeability Determination: Application to Glucose

Chrystel Faure,* Frédéric Nallet,* Didier Roux,* Scott T. Milner,† Fabienne Gauffre,‡ David Olea,* and Olivier Lambert§

*Centre de Recherche Paul-Pascal (Centre National de la Recherche Scientifique), UPR 8641, Pessac, France; †ExxonMobil Research and Engineering, Annandale, New Jersey; ‡Interactions Moléculaires et Réactivite Chimique et Photochimique, UMR 5623, Université Paul-Sabatier, Toulouse, France; and §Imagerie Moléculaire et Nano-Bio-Technologie, Institut Européen de Chimie et Biologie, Université Bordeaux-1, Talence, France

ABSTRACT The glucose permeability of bilayers formed from phosphatidylcholine, Brij30, and sodium octadecyl sulfate has been determined via an enzymatic reaction. Glucose is encapsulated in either uni- or multilamellar vesicles (MLV) and its concentration in the dispersion medium is monitored by spectrophotometry analysis through the rate of glucose oxidase-catalyzed reaction of glucose oxidation. A kinetic model of leakage, taking explicitly into account one, two, or n_w-walls ($n_w \gg 1$) for the vesicles and assuming an enzymatic Michaelis-Menten behavior, is proposed and used to fit the experimental data. The two-wall model was chosen to fit experimental data obtained on MLV since an average value of 1.7 bilayers was estimated for MLV by cryo-TEM imaging. A permeability value of $5.8 \pm 4.4\ 10^{-9}$ cm/s was found. The proposed model is validated by the measurement of the bilayer permeability deduced from the modeling of glucose leakage from unilamellar vesicles with the same composition. In this latter case, a value of $8.3 \pm 0.7\ 10^{-9}$ cm/s is found for the permeability, which is within the error bar of the value found with MLV.

INTRODUCTION

For more than 30 years, the estimation of bilayer permeability to different types of solutes has been of great interest for biophysicists, especially for phospholipid-based membranes. One of the reasons for such an interest is that phospholipid vesicles or liposomes (uni- or multilamellar) are regarded as potential drug delivery systems, e.g., vectors for gene transfer (1,2), in the diagnostic imaging of tumors (3), or as cosmetic agents for the delivery of moisturizers and antiinflammatory agents to the skin (4).

Most of the time, membrane permeabilities of liposomes are not calculated but discussed from the comparison of the time-dependent release of a solute which can easily be traced or from the comparison of the percent efflux of the solute measured at a given time. Such comparative studies have been performed to assess the effect of temperature (5,6), sterols (5–9), liposome coatings (10), phospholipid type (11), addition of amphiphilic compounds (12), or proteins (13,14) on bilayer permeability to a given molecule. If this solute is a dye (carboxyfluorescein (8,10), calcein (12,14)), its release is determined by monitoring the increase of fluorescence intensity accompanying the dilution of self-quenched fluorophores into the surrounding medium. In the case of enzyme substrate such as glucose, its loss is followed spectrophotometrically by an enzyme assay, usually hexokinase and glucose-6-phosphate dehydrogenase (5–7,11,13,15,16).

More recently, a method based on the measurement of the time-dependence of the second harmonic field produced by light irradiation of a liposome suspension in the presence of malachite green was developed. The fitting of the decay of the second harmonic field leads to the determination of time constants, which are discussed in term of liposome permeability (17,18). This technique may be adapted to many systems (polymer beads, emulsions, etc.) (17), but it is specific to one solute, namely the malachite green.

The first calculation of permeability dates back from 1969 when Johnson and Bangham (19) proposed a method to measure permeability coefficients for a single-walled system, i.e., unilamellar vesicles. A radioactive tracer (e.g., $^{42}K^+$) is encapsulated in unilamellar liposomes placed in dialysis bags, with the bags themselves placed in tubes containing isotope-free solutions. The counts escaping from the liposomes have to pass through the bag into the external solution where the radioactivity counting is then performed at known times. A mathematical model is presented which allows the calculation of the permeability coefficient of liposomes knowing the bags permeability and volume, the liposome volume, and the number of counts in the external solution. This method has been largely used for determination of the permeability coefficient to alkali metal cations (K^+, Na^+ (20–22), Cl^- (21), and Cs^+ (22)) and ^{14}C glucose (21,23–25), but is not straightforward and requires labeled solutes.

Radioactivity measurements have also proved to be efficient in the case of black lipid membranes. Wood et al. (26) showed that the permeability value of a planar film could be deduced from the counts of labeled material that passes through the black lipid films. The permeability to ^{14}C glucose was found, e.g., for lipid extract of blood cells (26,27)

Submitted May 3, 2006, and accepted for publication August 28, 2006.

Address reprint requests to C. Faure, Tel.: 33-556-84-56-65; E-mail: faure@crpp-bordeaux.cnrs.fr.

Didier Roux's present address is Saint-Gobain-Les Miroirs, 18 Avenue d'Alsace, F-92096 La Défense Cedex, France.

0006-3495/06/12/4340/10 $2.00

doi: 10.1529/biophysj.106.088401

and phosphatidylcholine-containing films (28,29). One of the major drawbacks of this technique is that preparation of the bimolecular lipid membranes results from the brushing of a solution containing organic solvents in which lipids are dissolved: the exact composition of the membranes is thus not known, and additional organic molecules are present to some extent in the black films.

All the above reported techniques for permeability coefficient measurements require labeled molecules, are discrete methods, and rely on mathematical models developed for uni-lamellar vesicles. In this article, we report a real-time, one-step method to calculate the permeability coefficient to isotope-free solutes across bilayers based on the time-dependence of the external solute concentration. Mathematical models for solute release from two-wall and multiwall systems are proposed that allow the determination of membrane permeability. The two-wall model is applied to the release of glucose through multilamellar vesicles. In our case, the extravesicular glucose concentration was indirectly followed by the measurement of the time-dependence of the rate of glucose oxidation through an enzymatic assay. Cryo-TEM imaging shows that glucose-containing vesicles are two-walled vesicles and the corresponding model leads to a value of the glucose permeability, which is compared to the value obtained from unilamellar vesicles of the same composition. The latter value is deduced from a one-wall model based on the work of Sato et al. (30). Both values are found to be comparable, which confirms the validity of the proposed model.

MATERIALS AND METHODS

Chemicals and solutions

A mixture of phosphatidylcholine from fat-free soybean lecithin consisting mainly of linoleic phosphatidylcholine (Lipoid S100) was provided by Lipoid (Ludwigshafen, Germany). A mixture of dodecyl-polyoxyethyleneglycols $C_{12}E_n$ in which $n \approx 4$ (Brij30), and sodium octadecyl sulfate (SOS), were purchased from Aldrich (Milwaukee, WI).

The glucose oxidase (GOx) from *Aspergillus niger* (E.C.1.1.3.4, type VII-S) was obtained from Sigma (St. Louis, MO). Peroxidase from horseradish (Grade II) as well as 2,2′-azino-bis(3-ethylbenzthiazoline-6-sulfonic acid) (ABTS) was from Boehringer Mannheim (Mannheim, Germany). *D*-(+)-glucose was purchased from Sigma. A potassium phosphate buffer (0.1 M, pH = 7) was obtained by adjusting the pH of a solution of K_2HPO_4, $3H_2O$ (2.28 g/100 mL water) to 7.0 by adding a solution of KH_2PO_4 (1.36 g/100 mL water). *D*-(+)-glucose (1.1 mM) and peroxidase (POD, 1.58 U/mL) were dissolved in water, whereas ABTS (1.6 mM) and GOx were dissolved in phosphate buffer. The *D*-(+)-glucose solution was left to mutarotate at room temperature for at least 24 h before use.

The molecular weight of glucose oxidase is 150 kDa. In all experiments, unless otherwise specified, 1 g of GOx contains 185,000 U. One unit (U) is the amount of enzyme required to oxidize 1 μmol of β-*D*-glucose per minute at 35°C and pH = 5.1 (Sigma definition).

Preparation of vesicle dispersions

Preparation of surfactant mixtures

SOS and S100 powders were first separately lyophilized to remove all water traces. Each surfactant was weighed in the right proportion—Brij30 (5 wt % of total surfactants), SOS (20 wt %), and S100 (75 wt %)—to give a total amount of 50 mg and then dissolved in chloroform/methanol (4/1 v/v). All the fractions were mixed together and the organic solvents were removed under vacuum using a rotavapor. Then, water and organic solvent traces were removed by overnight lyophilization.

Preparation of multilamellar vesicles (MLV)

Multilamellar vesicles (MLV) were obtained from a lamellar phase prepared by mixing surfactants and a *D*-(+)-glucose solution in equal amounts. Fifty milligrams of a 0.275 M glucose solution was added to hydrate 50 mg of the yellowish surfactant mixture. The sample was then manually sheared at room temperature for ~10 min and left without stirring for 10 additional minutes. This step was repeated until the paste looked homogeneous. A compact phase of multilamellar vesicles is then obtained. Twenty milligrams of MLV were then dispersed into an O_2-saturated ABTS solution (2.215 mL) under agitation using a vortex stirrer (600 rpm) for ~10 min. This step was performed just before spectrophotometric measurements.

Preparation of unilamellar vesicles (UV)

Thirty milligrams of lyophilized surfactants—Brij30 (5 wt % of total surfactants), SOS (20 wt %), and S100 (75 wt %)—are dissolved in 2 mL chloroform. The organic solvent is removed by rotary evaporation for 2 h, leaving a thin film on the 25 mL round-bottomed flask wall. The dried film is then rehydrated with 1.470 mL of ABTS solution in phosphate buffer (pH = 7) and 30 μL of a 0.275 M *D*-(+)-glucose solution. The milky solution obtained after flask-stirring is then poured into a vial and sonicated at 30% power in a Branson Sonifier 250 Ultrasonic Model (duty cycle 80%) for 20 min (Branson Ultrasonics, Danbury, CT). The sample was sealed during sonication, and immersed in an icy water bath to avoid any heating of the solution. Sonication was performed just before spectrophotometric measurements. The absence of any MLV in the sonicated solution was checked by phase contrast microscopy analysis.

Vesicle radius measurement

The size distribution of the multilamellar vesicles was determined by static light scattering using a Malvern Autosizer model S (Malvern Instruments, Malvern, Worcestershire, United Kingdom).

Unilamellar vesicles radius was measured using dynamic light scattering. Measurements were made at a scattering angle of 90° and the sample was maintained at 20 ± 1°C. The laser wavelength was 6471 Å.

Glucose oxidase activity measurement

Glucose oxidase (GOx) activity, i.e., the reaction rate of the glucose oxidase-catalyzed reaction, was assayed using a spectrometric procedure provided by Boehringer Mannheim. This method is a modification of a previously described method where O-dianisine was used as the leuco-dye instead of ABTS (DH_2) (31,32). The assays are based on the redox reactions

$$D(+)\text{Glucose} + O_2 \overset{\text{GOx}}{\Longleftrightarrow} D\text{-glucono-1, 5-lactone} + H_2O_2$$

$$H_2O_2 + DH_2 \overset{\text{POD}}{\Longleftrightarrow} 2H_2O + D,$$

where D, the oxidized form of ABTS (DH_2), is a dye ($\lambda_{abs} = 405$ nm).

The reaction rate of the glucose oxidase-catalyzed reaction is therefore determined by measuring the increase in absorbency at 405 nm resulting from ABTS oxidation through a peroxidase (POD)-coupled system as a function of time. All the experiments were performed using a Perkin-Elmer UV-visible spectrophotometer (Perkin-Elmer, Boston, MA). The temperature

of the spectrophotometer cell (25°C) was kept constant using flowing water. For MLV measurements, the 0.1 cm light-path cell was filled with ABTS (1.6 mM in the cell), POD (1.58 U mL^{-1} in the cell), GOx (50 mU mL^{-1} in the cell), and glucose-containing multilamellar vesicles (20 mg in 2.5 mL, i.e., a glucose concentration of 1.1 mM in the cell). Oxygen was provided by the solution of ABTS, which was oxygen-saturated before each measurement. Experiments were carried out at pH = 7.

For experiments performed on unilamellar vesicles, 1-cm light-path cells were preferred. Concentrations in POD and GOx in the cell are similar to those used for MLV experiments, while ABTS concentration is slightly lower, but still in excess (1.3 mM in the cell). Five-hundred microliters of the SUV dispersions in ABTS (see Preparation of Unilamellar Vesicles) were put into the cell filled with ABTS, POD, and GOx, so that a glucose concentration of 1.1 mM is also reached in the spectrophotometer cell.

THE MODEL

Kinetic model of leakage: concentration of glucose in the outer phase

One-wall (unilamellar) vesicles

A model for solute permeability through one single bilayer, appropriate for unilamellar vesicles, has been proposed by Sato et al. (30). Here, we simply recall the main concepts and equations, as they will prove useful for the proposed generalizations in the following.

Let us consider a compound simultaneously present inside and outside an unilamellar vesicle. Let us call $c_{in}(t)$ and $c_{out}(t)$ its concentrations, respectively, which are inside and outside the single-walled vesicle, and V_{out} the volume of outer phase. By definition of the membrane permeability P, the variation $\delta c_{out}(t)$ of $c_{out}(t)$ during the delay δt is given by the equation (19,22)

$$V_{out}\delta c_{out}(t) = \frac{SP}{2}[c_{in}(t) - c_{out}(t)]\delta t, \quad (1)$$

where S denotes the sum of the outer and inner surface area of the liposomal membrane.

Taking into account mass balance (i.e., expressing that the total number of solute molecules, either inside the vesicle or in the outer medium, is a constant), the two concentrations are related by

$$V_{out}c_{out}(t) + V_{in}c_{in}(t) = V_{tot}c_{tot}, \quad (2)$$

with (in the limit where the volume encapsulated by the vesicle is much smaller than the volume of the outer medium, that is to say, $V_{in} \ll V_{out}$),

$$c_{in}(t) = \frac{V_{out}}{V_{in}}[c_{tot} - c_{out}(t)]. \quad (3)$$

Written as a differential equation, Eq. 1 then takes the form

$$\frac{d[c_{out}(t)/c_{tot}]}{dt} = \frac{SP}{2V_{in}}\left[1 - \frac{c_{out}(t)}{c_{tot}}\right]. \quad (4)$$

The solution of Eq. 4 is easily expressed as a single-exponential relaxation, and written as

$$c_{out}(t) = c_{tot} + [c_{out}(0) - c_{tot}]\exp[-t/\tau], \quad (5)$$

with the characteristic time for leakage out of the vesicle being given by

$$\tau = \frac{2V_{in}}{SP}. \quad (6)$$

Besides, note that Eq. 5 implies that $c_{out}(\infty) \equiv c_{out}^{\infty} = c_{tot}$, a relation to be used below, in Results.

In the case of a spherical vesicle of outer-radius R and wall-thickness δ, the geometrical factor in Eq. 6 is given by

$$\frac{V_{in}}{S} = \frac{1}{3}\frac{[R-\delta]^3}{R^2 + [R-\delta]^2}, \quad (7)$$

which leads, in the limit where $\delta \ll R$, to a characteristic time of leakage expressed for unilamellar vesicles as

$$\tau = \frac{R}{3P}. \quad (8)$$

Multiwall vesicles

The kinetic equation for one-wall vesicles, Eq. 1, is easily generalized to the case of multiwall vesicles, with n_w inner compartments and, therefore, n_w+1 concentration variables. Indeed, the total number of solute molecules contained in the i^{th} compartment, with a volume V_i, varies because matter transfers occur with the two adjacent compartments $i+1$ and $i-1$, through permeation across the two bilayer walls of mean areas S_i and S_{i-1}, respectively (refer to the schematic drawing in Fig. 1; note also that, as compared to the conventions used in writing Eq. 1, we have dropped here a factor 2). Assuming that the permeability coefficient P does not depend on the wall rank i, such a mechanism leads to

$$V_i\frac{dc_i(t)}{dt} = P[S_{i-1}[c_{i-1}(t) - c_i(t)] - S_i[c_i(t) - c_{i+1}(t)]], \quad (9)$$

since a more concentrated compartment will always leak into a less concentrated one. Consider, however, that Eq. 9 is valid only for $1 < i < n_w + 1$, and should be replaced for the outer and innermost compartments by, respectively,

$$V_{out}\frac{dc_{out}(t)}{dt} = PS_{n_w}[c_{n_w}(t) - c_{out}(t)] \quad (10)$$

and

$$V_1\frac{dc_1(t)}{dt} = PS_1[c_1(t) - c_2(t)]. \quad (11)$$

It is also important to realize that, owing to mass balance, Eqs. 9–11 are not independent. The overall number of solute molecules, either entrapped inside the multiwall vesicle or freely distributed in the outer medium, should be a constant:

$$\sum_{i=1}^{n_w} V_i c_i(t) + V_{out}c_{out}(t) = V_{tot}c_{tot}. \quad (12)$$

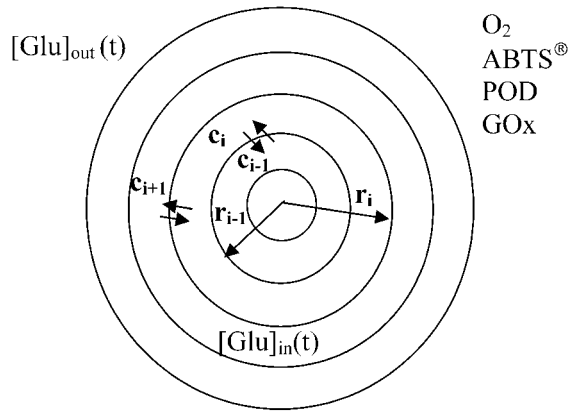

FIGURE 1 Schematic representation of a multilamellar vesicle in the assay medium.

The solution of the kinetic equations is not easily obtained in the most general case and we shall now consider, for illustration purposes, two relevant limiting situations—namely, a very large and homogeneous multiwall vesicle, as well as a two-wall vesicle with an inner compartment of arbitrary volume.

Large multiwall vesicles

For simplicity, we assume below that the bilayer thickness δ is much smaller than other characteristic lengths of the multiwall vesicle. Describing the i^{th} compartment of the vesicle as a spherical shell with inner and outer radii, respectively, r_{i-1} and r_i, Eq. 9 may then be written as

$$\frac{dc_i(t)}{dt}=P\left[\left[\frac{3r_{i-1}^2}{r_i^3-r_{i-1}^3}\right][c_{i-1}(t)-c_i(t)]+\frac{3r_i^2}{r_i^3-r_{i-1}^3}[c_{i+1}(t)-c_i(t)]\right]. \tag{13}$$

For a large number of bilayers ($n_w \gg 1$), the concentration variation from compartment to compartment will be very gradual, meaning that a continuous rather than discrete description should be adequate. Replacing $c_i(t)$ by its continuous counterpart $c(r,t)$ (refer to the Appendix for technical details), the following form of Eq. 13 is then obtained as

$$\frac{\partial c(r,t)}{\partial t}=Pd\left[\frac{2}{r}\frac{\partial c(r,t)}{\partial r}+\frac{\partial^2 c(t,r)}{\partial r^2}\right], \tag{14}$$

where d is the period of the bilayer stack in the multiwall vesicle. As a matter of fact, Eq. 14 is classically used to describe a spherically symmetric diffusion process through a continuous body, and one might have then begun with Eq. 14, appealing to a continuum description at the outset. The identification of Pd as the three-dimensional diffusion coefficient is physically evident, in that a diffusive current $Pd\nabla c$ is the continuum limit of $J = P\ (c_{i+1}-c_i)$. Moreover, the characteristic time, defined by

$$\tau_w=\frac{R^2}{Pd}=3n_w\tau, \tag{15}$$

appears as the natural timescale for the leakage process, where R (identical to r_w in the discrete limit) is the outer radius of the multiwall vesicle and n_w is the number of bilayers, such that $n_w d = R$. Indeed, as detailed in the Appendix, the solution of Eq. 14 for an initially uniform distribution of the solute within the multiwall vesicle is found to be given by

$$c(r,t)=A+B\sum_{q=1}^{\infty}(-1)^{q+1}\frac{\sin(q\pi r/R)}{q\pi r/R}\exp\left[-q^2\pi^2\frac{t}{\tau_w}\right], \tag{16}$$

where A and B are constant parameters, to be determined by the boundary conditions.

Mass balance of the solute, Eq. 12, together with the inequality $V_{out} \gg V_{in}$, leads to a relation essentially identical to Eq. 3, obtained with a single-wall vesicle, namely,

$$c_{out}(t)=c_{tot}-\frac{V_{in}}{V_{out}}c_{in}(t). \tag{17}$$

In terms of the total, c_{tot}, and mean solute concentration $c_{in}(t)$ within the multiwall vesicle, the latter is now given by the integral,

$$c_{in}(t)=\frac{\int c_{in}(r,t)4\pi r^2 dr}{4\pi R^3/3}=A+3B\sum_{q=1}^{\infty}\frac{1}{q^2\pi^2}\exp\left[-\frac{q^2\pi^2 t}{\tau_w}\right]. \tag{18}$$

The two integration constants A and B then obtain from the second part of Eq. 18, since $c_{in}(\infty)=A$ and $c_{in}(t=0)=A+B/2$, which, taking into account Eq. 17, finally leads to the required solute concentration outside the multiwall vesicle:

$$c_{out}(t)=c_{out}^{\infty}-6[c_{out}^{\infty}-c_{out}(0)]\sum_{q=1}^{\infty}\frac{1}{q^2\pi^2}\exp\left[-\frac{q^2\pi^2 t}{\tau_w}\right]. \tag{19}$$

Note that, at contrast with the single-exponential relaxation, Eq. 5, obtained with one-wall vesicles, the leakage of the solute through a multiwall vesicle is described, in the continuous limit, by an infinite series of exponential modes. The slowest mode has a relaxation time given by τ_w/π^2, or $3n_w\tau/\pi^2$, and is, as expected physically, much longer than τ for an object of the same outer dimensions in the limit of a large number of bilayer walls, $n_w \gg 1$.

Two-wall vesicles

The continuous limit obviously fails in describing multiwall vesicles with a few walls. It is also inappropriate for heterogeneous vesicles, for instance when the innermost compartment is large compared to compartments sandwiched in-between two bilayers. This is the reason why we consider again the kinetic problem described by Eq. 9 and following in the two-wall limit, $n_w = 2$. Eliminating the variable $c_{out}(t)$ in Eq. 10 with the help of mass balance, and as before considering V_{out} much larger than the total volume encapsulated by the vesicle, we arrive at

$$\frac{dc_1(t)}{dt} = -\frac{PS_1}{V_1}[c_1(t) - c_2(t)]$$
$$\frac{dc_2(t)}{dt} = \frac{PS_1}{V_2}c_1(t) - \frac{P[S_1 + S_2]}{V_2}c_2(t) + \frac{PS_2}{V_2}c_{tot}. \quad (20)$$

There are thus exactly two modes in the relaxation behavior of any of the three concentration variables $c_1(t)$, $c_2(t)$, or $c_{out}(t)$, with characteristic frequencies given by the eigenvalues of the kinetic matrix K defined by

$$K = \frac{PS_1}{V_1}\begin{bmatrix} 1 & -1 \\ -\frac{V_1}{V_2} & \frac{V_1[1 + S_2/S_1]}{V_2} \end{bmatrix}. \quad (21)$$

Introducing τ_2 as $V_1/(PS_1)$ and the volume and area ratios as $v_{12} = V_1/V_2$ and $s = S_2/S_1$, the two relaxation times are thus explicitly given by

$$\tau_+ = \frac{2\tau_2}{1 + v_{12}[1 + s] + \sqrt{1 + 2v_{12}[1 - s] + v_{12}^2[1 + s]^2}}$$
$$\tau_- = \frac{2\tau_2}{1 + v_{12}[1 + s] - \sqrt{1 + 2v_{12}[1 - s] + v_{12}^2[1 + s]^2}}. \quad (22)$$

It is then somewhat tedious but straightforward to express the solution of Eq. 20, in the case of an initially homogeneous distribution of solute inside the two-wall vesicle, as

$$c_{out}(t) = c_{out}^{\infty} + \frac{c_{out}^{\infty} - c_{out}(0)}{\tau_+ - \tau_-}\left\{\tau_+\left[\frac{\tau_2}{(1 + v_{12})\tau_+} - 1\right]\right.$$
$$\left.\exp(-t/\tau_+) + \tau_-\left[1 - \frac{\tau_2}{(1 + v_{12})\tau_-}\right]\exp(-t/\tau_-)\right\}. \quad (23)$$

Enzymatic reaction rate

For a Michaelis-Menten enzyme such as glucose oxidase (33–35), the enzyme-catalyzed reaction rate can be expressed as a function of the substrate concentration, i.e., *D*-(+)- glucose concentration, as (36)

$$v(t) = \frac{v_m[Glu]_{out}(t)}{K_m + [Glu]_{out}(t)}. \quad (24)$$

In this equation, $[Glu]_{out}(t)$ denotes the outside concentration in glucose, v_m is the maximal reaction rate for a given enzyme concentration, i.e., the reaction rate at large substrate concentration, and K_m, the so-called Michaelis constant, is the substrate concentration that results in half-maximal rate.

When $[Glu]_{out} \ll K_m$ as in our conditions, Eq. 24 can be simplified as

$$v(t) = \frac{v_m[Glu]_{out}(t)}{K_m}. \quad (25)$$

We can now simply express the time-dependent rate of the GOx-catalyzed reaction of glucose oxidation for one-, two-, and multiwall vesicles, from Eqs. 5, 23, and 19, respectively.

One-wall vesicles

The reaction rate is described by the following, single-mode relaxation equation:

$$v(t) = \frac{v_m}{K_m}\left[[Glu]_{tot} + ([Glu]_{out}^0 - [Glu]_{tot})\exp\left(-\frac{t}{\tau}\right)\right]. \quad (26)$$

Two-wall vesicles

Two modes should be observed in the reaction rate,

$$v(t) = \frac{v_m}{K_m}\left[[Glu]_{out}^{\infty} + \frac{[Glu]_{out}^{\infty} - [Glu]_{out}^0}{\tau_+ - \tau_-}\right.$$
$$\times\left[\tau_+\left[\frac{\tau_2}{(1 + v_{12})\tau_+} - 1\right]\exp(-t/\tau_-)\right.$$
$$\left.\left. + \tau_-\left[1 - \frac{\tau_2}{(1 + v_{12})\tau_-}\right]\exp(-t/\tau_-)\right]\right], \quad (27)$$

with a quasi-single-mode behavior recovered in the long time limit when the short-lived mode, with relaxation time τ_+, has eventually decayed to negligible values.

Multiwall vesicles

There are an infinite number of modes in the continuous limit, as expressed by

$$v(t) = \frac{v_m}{K_m}\left[[[Glu]_{out}^{\infty} - 6([Glu]_{out}^{\infty} - [Glu]_{out}^0)]\sum_{q=1}^{\infty}\frac{1}{(q\pi)^2}\right.$$
$$\left.\exp\left(-q^2\pi^2\frac{t}{\tau_w}\right)\right], \quad (28)$$

with, as previously with two-wall vesicles, a quasi-single-mode behavior recovered in the long-time limit when all modes, except the one with rank $q = 1$, have decayed to negligible values.

RESULTS

Model validity

The models developed in the previous section for one-, two-, or multiwalled systems are valid as long as

1. The time-dependence of $[Glu]_{out}(t)$ is only due to the glucose leakage kinetics and not to the enzymatic reaction, which consumes glucose with time. To check that assumption, the reaction rate of a MLV-free solution containing 1.1 mM glucose, was measured. This value is the maximum glucose concentration when all encapsulated glucose molecules have leaked from MLV. The time-dependent absorbency (*open symbols*), as well as its time derivative (*solid symbols*), i.e., the reaction rate for this concentration, are plotted in Fig. 2 for a solution containing GOx (50 U/L). One sees that the reaction rate

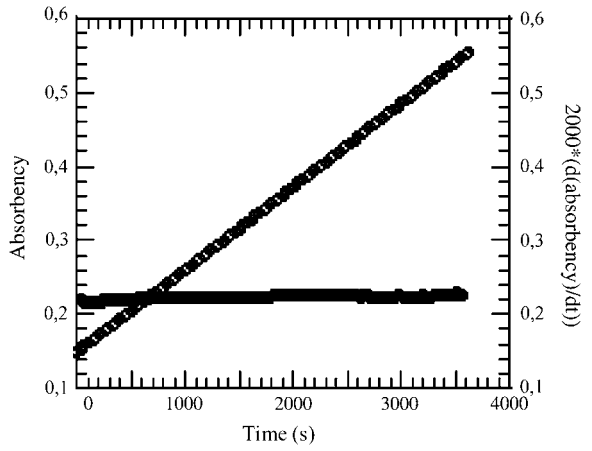

FIGURE 2 Spectrophotometric response of a solution of glucose (1.1 mM) in phosphate buffer containing glucose oxidase (50 U L^{-1}), peroxidase (1.58 U mL^{-1}), and ABTS (1.6 mM). (*Open circles*) Absorbency of the solution measured at $\lambda = 405$ nm as a function of time. (*Solid circles*) Glucose oxidase-catalyzed reaction rate as a function of time.

remains constant over ~3500 s, which means that the concentration of glucose can thus be considered as constant on the experimental timescale, as assumed in the previous section.

2. The extravesicular concentration of glucose remains low enough for the reaction rate to be glucose-dependent, i.e., the reaction rate must differ from the constant value v_m, which occurs when $[Glu]_{out} \gg K_m$ (see Eq. 24). This is confirmed by Fig. 3 *b* where the reaction rate obtained when glucose is encapsulated (*solid symbols*) is plotted as a function of time. This plot results from the derivation of the spectrophotometric data given in Fig. 3 *a*. The continuous increase of the enzymatic reaction rate $v(t)$, obtained when glucose is initially encapsulated, shows the leakage of this compound through the vesicles.
3. The size polydispersity is not too large. Obviously, the kinetic equations refer to a single vesicle, whereas the experiments always involve a population of vesicles, with the subsequent serious limitation that the size distribution will smear out the values for the fitting parameters. Size polydispersity remains small in the present study for unilamellar vesicles. However, it should be kept in mind that, in our experiments with two-wall vesicles, the geometrical parameters are somewhat more broadly distributed.

Unilamellar vesicles: modeling and permeability measurement

Fig. 4 displays the fitting of the experimental reaction rate (*open circles*) with Eq. 26. In this fit, $\frac{v_m}{K_m}$ value was fixed to the theoretical value 1.10^{-4} ΔAbs/mM/s (37), while $[Glu]^0_{out}$, $[Glu]_{tot}$, and τ are adjustable parameters. From this fit, a value of 1.15 ± 0.01 mM can be extracted for $[Glu]_{tot}$, which is very close to the experimental value, namely 1.1 mM.

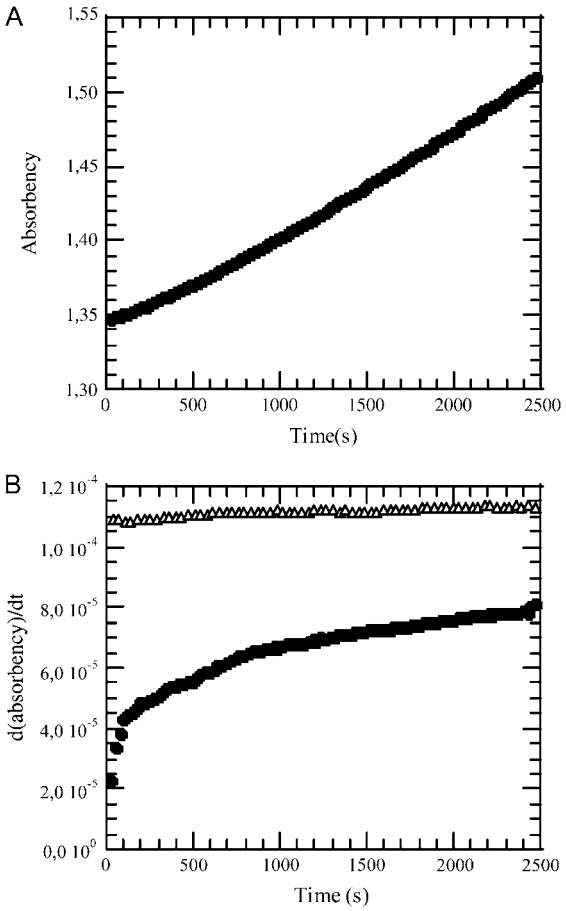

FIGURE 3 (*a*) Spectrophotometric response ($\lambda = 405$ nm) of a dispersion of glucose-containing MLV (20 mg/2.5 mL) in phosphate buffer containing glucose oxidase (50 U L^{-1}), peroxidase (1.58 U mL^{-1}), and ABTS (1.6 mM). Glucose concentration in the spectrometric cell is 1.1 mM. (*b*) Glucose oxidase-catalyzed reaction rates as a function of time when glucose is encapsulated in MLV (*circles*) or not (*triangles*).

Fixing this parameter to such a value would not have changed the fit quality. Besides, the initial concentration of glucose outside liposomes—which cannot be precisely known from the preparation protocol—is found to be 0.23 ± 0.01 mM. A characteristic time, τ of 158 ± 5 s, is found. From Eq. 8, one can deduce the permeability coefficient of a bilayer knowing the vesicle radius. The radius R was found to be 39 ± 2 nm by dynamic light scattering, which leads to a value for the permeability P of 8.3 ± 0.7 10^{-9} cm/s.

Multiwall vesicles

Cryo-TEM imaging

Fig. 5 shows typical images of MLV in which glucose was encapsulated observed by transmission electronic microscopy. These MLV were dispersed in the assay medium for imaging. One can notice that the lamellarity of the vesicles is poor, probably because the osmotic pressure of the glucose solution tends to disrupt the vesicles. From cryo-TEM

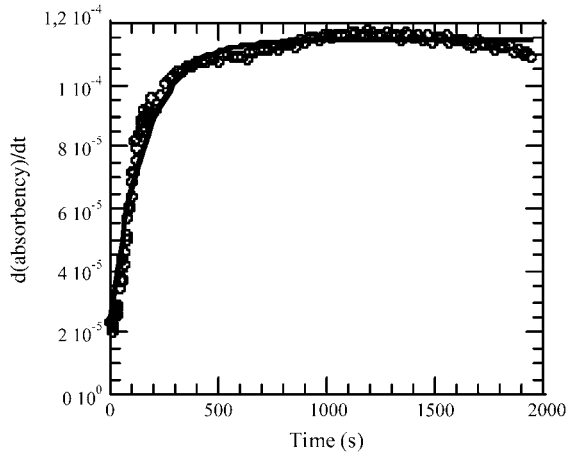

FIGURE 4 Modeling of the rate of the glucose oxidase catalyzed-reaction when glucose leaks from unilamellar vesicles, using Eq. 26. The experimental data are symbolized by open circles; the model appears in solid line representation. Fixed parameter: $\frac{v_m}{K_m} = 0.0001\ \Delta\text{Abs mM}^{-1}\ \text{s}^{-1}$. Adjustable parameters are $[\text{Glu}]^0_{\text{out}} = 0.7\,\text{mM}$, $\tau = 1000\,\text{s}$, and $[\text{Glu}]^\infty_{\text{out}} = 1.1\,\text{mM}$.

images, we estimated that the average number of bilayers which compose the MLV is 1.7 (175 vesicles were considered), with the distribution indeed peaked at two bilayers. Two-wall vesicles are indicated by arrows in Fig. 5. Moreover, an important point is also that the ratio between the inner volume (V_1) and the volume of the external compartment (V_2), assuming a spherical shape, is roughly constant. The volume ratio v_{12} in Eqs. 22 and 23 can then be estimated from these images to a value 1.05. The surface ratio s, however, has a much wider distribution because the outer bilayer is sometimes significantly crumpled.

Modeling

Fig. 6 displays the fitting of the experimental reaction rate (Fig. 3 *b*) with Eq. 27, i.e., assuming a two-wall vesicle. The values for v_m and K_m were fixed to the experimental values measured in previous studies (37), namely 0.0025 ΔAbs s^{-1} and 25 mM, respectively. All the other parameters, namely $[\text{Glu}]^0_{\text{out}}$, $[\text{Glu}]^\infty_{\text{out}}$, τ_2, v_{12}, and s, were considered as freely adjustable ones. From the best fit, τ_2 was found to be 1160 $\pm$ 12 s. A value of 0.98 $\pm$ 0.02 for v_{12} can also be extracted, with s equal to 26 $\pm$ 0.7. This corresponds to short and long relaxation times (as defined in Eq. 22), $\tau_+ = 44$ s and $\tau_- =$ 1205 s, respectively. While the value for v_{12} is in good agreement with the experimental value estimated by cryo-TEM imaging (see previous section), the large value for s cannot be accounted for without assuming a significant crumpling of the outer bilayer; it is indeed sometimes observed in cryo-TEM (see Fig. 5). Finally, a value of 0.871 $\pm$ 0.001 mM for $[\text{Glu}]^\infty_{\text{out}}$ (respectively, 0.046 $\pm$ 0.004 mM for $[\text{Glu}]^0_{\text{out}}$) is deduced from the fitting procedure. The $[\text{Glu}]^\infty_{\text{out}}$ value is a bit lower than the expected one (1.1 mM), and a definitely worse fit would result from fixing $[\text{Glu}]^\infty_{\text{out}}$ to such a value. As a tentative explanation for this discrepancy, we

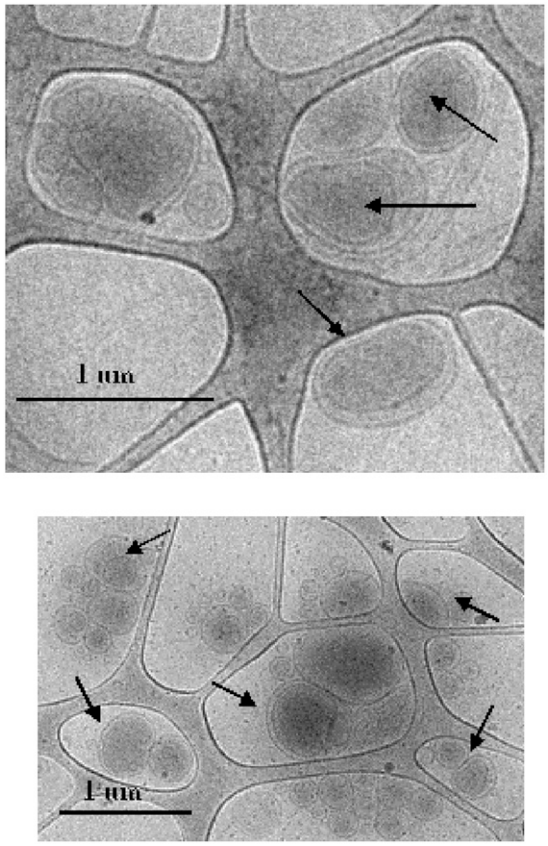

FIGURE 5 Cryo-TEM images showing glucose-containing multilamellar vesicles diluted in the assay medium. Arrows indicate MLV with two bilayers.

suggest that, owing to the much slower final kinetics obtained with MLV, we lack experimental data for a precise determination of the long-time limit of the reaction rate.

Permeability calculation

From the definition of τ_2 that follows Eq. 21, namely $\tau_2 = V_1/(PS_1)$, the bilayer permeability can be calculated. As inferred from cryo-TEM, the inner compartment is always close to being a sphere and we thus take $V_1/S_1 = 3r_1$. The radius r_1 itself is obtained from the overall size—expressed as a radius R—of the MLV, measured in static light scattering, together with the volume ratio v_{12}, deduced from either cryo-TEM or the fitting procedure, as $r_1 = R\sqrt[3]{\frac{v_{12}}{1+v_{12}}} \approx 0.8R$. The overall size was found to be $R =$ 0.25 $\pm$ 0.19 μm, with the large uncertainty resulting from the rather broad size distribution. Using the fitted value $\tau_2 =$ 1160 $\pm$ 12 s given above, a permeability coefficient $P =$ 5.8 $\pm$ 4.4 10^{-9} cm/s is eventually found.

DISCUSSION

Permeability coefficient of bilayers composed of phosphatidylcholine (75 wt %), sodium octadecyl sulfate (20 wt %)

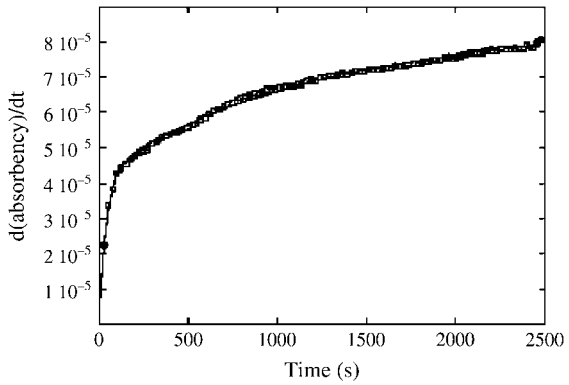

FIGURE 6 Modeling of the rate of the glucose oxidase catalyzed-reaction when glucose leaks from MLV, using Eq. 27. The experimental data are symbolized by open circles while the model appears in solid line representation. Fixed parameters are $K_m = 25$ mM and $v_m = 0.0025$ ΔAbs s^{-1}. Adjustable parameters are $[Glu]^0_{out} = 0.06$ mM, $[Glu]^\infty_{out} = 0.87$ mM, $\tau_2 = 1160$ s, $v_{12} = 0.98$, and $s = 25.7$.

and Brij30 (5 wt %) to glucose has been measured for one- or two-wall vesicles, treating in each case the experimental data with appropriate mathematical models. In addition, a model relevant for vesicles composed of a great number of bilayers ($n_w \gg 1$) has been proposed, but without being experimentally validated yet. Experiments are underway to address this.

The values found for one- and two-wall vesicles are nicely consistent: $8.3 \pm 0.7\ 10^{-9}$ and $5.8 \pm 4.4\ 10^{-9}$ cm/s were determined for uni- and multilamellar vesicles mainly consisting of two bilayers, respectively, which we consider as confirming the validity of the two-wall vesicle model. However, a large error bar is found for the permeability coefficient measured with MLV, originating mainly in the rather large polydispersity of these vesicles.

Both values for P are much larger than those usually obtained for glucose leakage from unilamellar vesicles: $1.03\ 10^{-11}$ cm/s for dipalmitoyl phosphatidylethanolamine liposomes at 25°C (23); $3.36\ 10^{-11}$ cm/s for dipalmitoyl phosphatidylcholine/phosphatidylinositol (91:9) liposomes at 25°C (24); $4.13\ 10^{-11}$ cm/s for phosphatidylserine liposomes at 36°C (21); and 6.810^{-12} cm/s for soy bean phosphatidylcholine liposomes (25). However, our value is not far from the reported values for glucose permeability through black lipid membranes: Wood et al. (26) found a permeability of 5.10^{-8} cm/s for bilayers formed from phospholipids extracts of human red cells, Ligdard and Jones (28) found $7.5\ 10^{-8}$ cm/s when bilayers were prepared from egg phosphatidylcholine and cholesterol, and a value of $2.8\ 10^{-7}$ cm/s was proposed by Kafka (29) for egg phosphatidylcholine planar membranes. Hence, even though the values measured on black membranes are different from each other, they are at least three orders-of-magnitude higher than those calculated from liposomes.

An important difference in both types of studied systems is that black lipid membranes are prepared by brushing an organic solution in which membrane-forming components are dissolved. Consequently, the exact composition of black lipid membranes is not really known and, above all, such membranes contain organic molecules (chloroform, methanol, α-tocopherol (26), n-dodecane (28,29)), which are known to increase membrane permeabilities. In our case, vesicles were prepared from a mixture containing 30 wt % of surfactants: 5 wt % of Brij30 (dodecyl polyoxyethylene glycol $C_{12}E_4$) and 25 wt % of sodium octadecyl sulfate. Surfactants have been extensively studied for their capacity to alter the structural organization of the lipids (38,39), which is directly related to the membrane fluidity and permeability (11). It has been shown, for instance, that $C_{12}E_8$ (which is close to the Brij30 chemical structure) can perturb membrane structure at subsolubilizing concentration (40). A steep increase in carboxyfluorescein efflux from lipid vesicles is observed through addition of neutral detergents at a concentration where the morphological integrity of mixed bilayer vesicles is still preserved (41), and surfactants are known to display antibacterial properties by increasing the permeability of bacterial cell walls (42). Therefore, it is actually not surprising to find a high permeability value for surfactant-containing vesicles.

CONCLUSION

We propose a model of molecule leakage from two-walled systems, inspired by an already published one (30). The model is validated comparing bilayer permeability from one- and two-wall liposomes. The reaction rate of the glucose oxidase-catalyzed oxidation of the glucose that leaks from vesicles was measured by spectrometric assay. The fitting of the time-dependence of the reaction rate with the given model allows the determination of two characteristic times of leakage and thus, of the membrane permeability. The permeability coefficient value found for two-wall vesicles is close to that found on unilamellar vesicles and is discussed in terms of membrane composition.

We also developed a model for vesicles made of a high number of bilayers ($n_w \gg 1$). Working with MLV of high lamellarity could be advantageous since the rates of solute transport are often so small that other effects, such as vesicle fusion followed by release of the vesicular contents, may obscure the signal of interest (22). In addition, the reproducibility of measured permeability for unilamellar vesicles is very poor because of the susceptibility of large liposomes to mechanical rupture (19). MLV are indeed much more stable than unilamellar vesicles when dispersed in aqueous phase and no fusion has ever been observed in these systems. This leads us to propose a one-step method to determine the permeability of a membrane to any small molecule. It merely consists in encapsulating this molecule inside multilamellar vesicles, which results in the slowing down of its leak proportionally to the number of bilayers, to measure, via, e.g., an enzymatic assay, the concentration of the molecule in the dispersion medium, and to fit the experimental data with the proposed model. Such experiments are currently underway.

APPENDIX

The time-dependence for a compound concentration within the i^{th} spherical shell of outer radius r_i can be expressed as (refer to Eq. 13)

$$\frac{dc_i(t)}{dt}=P\left[\frac{3r_{i-1}^2}{r_i^3-r_{i-1}^3}[c_{i-1}(t)-c_i(t)]+\frac{3r_i^2}{r_i^3-r_{i-1}^3}[c_{i+1}(t)-c_i(t)]\right]. \quad \text{(I)}$$

A continuous description is obtained by writing

$$\frac{c_i(t)-c_{i-1}(t)}{d}=\frac{\partial c_i(t,r)}{\partial r}, \quad \text{(II)}$$

together with

$$\frac{1}{d}\left(\frac{c_{i+1}(t)-c_i(t)}{d}-\frac{c_i(t)-c_{i-1}(t)}{d}\right)=\frac{\partial^2 c_i(t,r)}{\partial r^2}, \quad \text{(III)}$$

the distance between two consecutive bilayers being d.
Combining Eqs. II and III gives

$$c_{i+1}(t)-c_i(t)=d^2\frac{\partial^2 c_i(t,r)}{\partial r^2}+d\frac{\partial c_i(t,r)}{\partial r}. \quad \text{(IV)}$$

Moreover, considering a continuous description also leads to

$$r_i^2 d\equiv\int r^2 dr=\frac{r_i^3-r_{i-1}^3}{3}, \quad \text{(V)}$$

$$r_i d\equiv\int r dr=\frac{r_i^2-r_{i-1}^2}{2}. \quad \text{(VI)}$$

Introducing Eqs. II, III, IV, V, and VI in Eq. I then gives

$$\frac{\partial c(t,r)}{\partial t}=Pd\left(\frac{2}{r}\frac{\partial c(t,r)}{\partial r}+\frac{\partial^2 c(t,r)}{\partial r^2}\right). \quad \text{(VII)}$$

Eq. VII is identical to Eq. 14. It is easily solved by introducing a Fourier expansion for the product $r\cdot c(t,r)$ of the form

$$rc[r,t]=rA+\sum_{q=1}^{\infty}C_q(t)\sin(\pi qr/R), \quad \text{(VIII)}$$

since Eq. VII becomes for the Fourier modes

$$\frac{dC_q(t)}{dt}=-Pd\frac{\pi^2 q^2}{R^2}C_q(t) \quad \text{(IX)}$$

with an exponentially decaying solution for a mode of rank q

$$C_q(t)=C_q(0)\exp\left(-\pi^2 q^2\frac{t}{\tau_w}\right). \quad \text{(X)}$$

The characteristic relaxation time τ_w is given by

$$\tau_w=\frac{R^2}{Pd}=3n_w\tau. \quad \text{(XI)}$$

In terms of the outer radius of the multiwall vesicle R, bilayer permeability P, and smectic period d, recall that $n_w\equiv R/d$ is the total number of bilayers per multiwall vesicle, and τ is the characteristic relaxation time for a single-wall vesicle of radius R (see Eq. 8).

Inserting the Fourier modes, Eq. X, into Eq. VIII yields for the concentration field

$$c(r,t)=A+\sum_{q=1}^{\infty}C_q(0)\frac{\sin(\pi qr/R)}{r}\exp\left(-q^2\pi^2\frac{t}{\tau_w}\right). \quad \text{(XII)}$$

Since at time $t=0$ the concentration is assumed uniform within the MLV, namely $c(r,t=0)=c_0$, the mode amplitudes $C_q(0)$ should be such that

$$\int_0^R rc(r,t=0)\sin\left(\frac{\pi qr}{R}\right)dr=-R^2c_0\frac{(-1)^q}{\pi q}\equiv-R^2A\frac{(-1)^q}{\pi q}+\frac{R}{2}C_q(0), \quad \text{(XIII)}$$

with B, therefore, representing the combination $2(c_0–A)$,

$$C_q(0)=B\frac{R(-1)^{q+1}}{\pi q}. \quad \text{(XIV)}$$

The present form for the mode amplitude of rank q at time 0, together with Eq. XII, eventually yields to Eq. 16.

REFERENCES

1. Ross, P. C., M. L. Hensen, R. Supabphol, and S. V. Hui. 1998. Multilamellar cationic liposomes are efficient vectors for *in vitro* gene transfer in serum. *J. Liposome Res.* 8:499–520.
2. Mignet, N., A. Bup, C. Degert, B. Delord, D. Roux, C. Hélène, J. C. François, and R. Laversanne. 2000. The spherulites: a promising carrier for oligonucleotide delivery. *Nucleic Acids Res.* 28:3134–3142.
3. Torchilin, V. P., V. S. Trubetskoy, A. M. Milshteyn, J. Canillo, G. L. Wolf, M. I. Papisov, A. A. Bogdanov, J. Narula, B. An Khaw, and V. G. Omlyanenko. 1994. Targeted delivery of diagnostic agents by surface-modified liposomes. *J. Controlled Release.* 28:45–58.
4. Vanlerberghe, G. 1996. Liposomes in cosmetics: how and why? *In* Non-Medical Applications of Liposomes, Vol. IV. D. D. Lasic and Y. Barenholz, editors. CRC Press, Boca Raton, FL. 77–90
5. Inoue, K. 1974. Permeability properties of liposomes prepared from dipalmitoyl lecithin, dimyristoyl lecithin, egg lecithin, rat liver lecithin and beef brain sphingomyelin. *Biochim. Biophys. Acta.* 339:390–402.
6. Kraske, W., and D. B. Mountcastle. 2001. Effects of cholesterol and temperature on the permeability of dimyristoyl phosphatidylcholine bilayers near the chain melting phase transition. *Biochim. Biophys. Acta.* 1514:159–164.
7. Demel, R. A., K. R. Brickdorfer, and L. L. M. Van Deenen. 1972. The effect of sterol structure on the permeability of liposomes to glucose, glycerol and Rb^+. *Biochim. Biophys. Acta.* 255:321–330.
8. Bittman, R., S. Clejan, M. K. Jain, P. W. Deroo, and A. F. Rosenthal. 1981. Effects of sterols on permeability and phase transitions of bilayers from PC lacking acyl groups. *Biochemistry.* 20:2790–2795.
9. Ranadavine, G. N., and A. K. Lala. 1987. Sterol-phospholipid interaction in model membranes: role of C5–C6 double bond in cholesterol. *Biochemistry.* 26:2426–2431.
10. Sagrista, M. L., M. Mora, and M. Africa de Madariaga. 2000. Surface modified liposomes by coating with charged hydrophilic molecules. *Cell. Mol. Biol. Lett.* 5:19–33.
11. Kitagawa, T., K. Inoue, and S. Nojima. 1976. Properties of liposomal membranes composed of short-chain lecithins. *J. Biochem.* (*Tokyo*). 79: 1147–1155.
12. Gubernator, J., M. Stasiuk, and A. Kozubek. 1999. Dual effect of alkylresorcinols, natural amphiphilic compounds, upon liposomal permeability. *Biochim. Biophys. Acta.* 1418:253–260.
13. Kitagawa, T., K. Inoue, and S. Nojima. 1976. Effect of albumin and methylated albumin on the glucose permeability of lipid membranes. *J. Biochem.* (*Tokyo*). 79:1135–1145.

14. Davidsen, J., K. Jorgensen, T. L. Andresen, and O. G. Mouritsen. 2003. Secreted phospholipase A2 as a new enzymatic trigger mechanism for localised liposomal drug release and absorption in diseased tissue. *Biochim. Biophys. Acta.* 1609:95–101.

15. Demel, R. A., S. C. Kinsky, C. B. Kinsky, and L. M. van Deenen. 1968. Effects of temperature and cholesterol on the glucose permeability of liposomes prepared with natural and synthetic lecithins. *Biochim. Biophys. Acta.* 150:655–665.

16. Kinsky, S. C., J. A. Haxby, D. A. Zopf, C. R. Alving, and C. B. Kinsky. 1969. Complement-dependent damage to liposomes prepared from pure lipids. *Biochemistry.* 8:4149–4158.

17. Srivastava, A., and K. B. Eisenthal. 1998. Kinetics of transport across a liposome bilayer. *Chem. Phys. Lett.* 292:345–351.

18. Yan, E. C. Y., and K. B. Eisenthal. 2000. Effect of cholesterol on molecular transport of organic cations across liposome bilayers probed by second harmonic generation. *Biophys. J.* 79:898–903.

19. Johnson, S. M., and A. D. Bangham. 1969. Potassium permeability of single compartment liposomes with and without valinomycin. *Biochim. Biophys. Acta.* 193:82–91.

20. Hamilton, R. T., and E. W. Kaler. 1987. Ionic permeability of synthetic vesicles. *J. Colloid Interface Sci.* 116:248–255.

21. Papahadjopoulos, D., S. Nir, and S. Ohki. 1971. Permeability properties of phospholipid membranes: effect of cholesterol and temperature. *Biochim. Biophys. Acta.* 266:561–583.

22. Hamilton, R. T., and E. W. Kaler. 1990. Alkali metal ion transport through thin bilayers. *J. Phys. Chem.* 94:2560–2566.

23. Nikolova, A., and M. N. Jones. 1996. Effect of grafted PEG-2000 on the size and permeability of vesicles. *Biochim. Biophys. Acta.* 1304:120–128.

24. Nicholas, A. R., A. J. Scott, N. I. Kennedy, and M. N. Jones. 2000. Effect of grafted polyethylene glycol (PEG) on the size, encapsulation efficiency and permeability of vesicles. *Biochim. Biophys. Acta.* 1463:167–178.

25. Lossen, O. 1972. A sequential dialysis method for measuring permeability coefficients of phospholipid vesicles. *Biochim. Biophys. Acta.* 282: 31–39.

26. Wood, R. E., F. P. Wirth, and H. E. Morgan. 1968. Glucose permeability of lipid bilayer membranes. *Biochim. Biophys. Acta.* 163:171–178.

27. Jung, C. Y. 1971. Permeability of bimolecular membranes made from lipid extracts of human red cell ghosts to sugars. *J. Membr. Biol.* 5: 200–214.

28. Lidgard, G. P., and M. N. Jones. 1975. *D*-glucose permeability of black lipid membranes modified by human erythrocyte membrane fractions. *J. Membr. Biol.* 21:1–10.

29. Kafka, M. S. 1974. The effect of insulin on the permeability of phosphatidylcholine bimolecular membranes to glucose. *J. Membr. Biol.* 18:81–94.

30. Sato, T., M. Kijima, Y. Shiga, and Y. Yonezawa. 1991. Photochemically controlled ion permeability of liposomal membranes containing amphiphilic azobenzene. *Langmuir.* 7:2330–2335.

31. Bergmeyer, H. U. 1981. Methods of Enzymatic Analysis, Vol. 1. H. U. Bergmeyer, editor.

32. Huggett, A. S. T., and D. A. Nixon. 1957. Use of glucose oxidase, peroxidase, and O-dianisine in determination of blood and urinary glucose. *Lancet.* 273:368–370.

33. Swoboda, B. E. P., and V. Massey. 1965. Purification and properties of the glucose oxidase from *Aspergillus niger*. *J. Biol. Chem.* 240:2209–2215.

34. Broun, G., E. Selegny, S. Avrameas, and D. Thomas. 1969. Enzymatically active membranes: some properties of cellophane membranes supporting cross-linked enzymes. *Biochim. Biophys. Acta.* 185:260–262.

35. Tsuchida, T., and K. Yoda. 1981. Immobilization of glucose oxidase onto a hydrogen peroxide permselective membrane and application for an enzyme electrode. *Enzyme Microb. Technol.* 3:326–330.

36. Michaelis, L., and M. Menten. 1913. The kinetics of invertase activity. *Biochem. Z.* 49:333–369. [in German].

37. Olea, D., and C. Faure. 2003. Quantitative study of the encapsulation of glucose oxidase into multilamellar vesicles and its effect on enzyme activity. *J. Chem. Phys.* 119:6111–6119.

38. Helenius, A., and K. Simon. 1975. Solubilization of membranes by detergents. *Biochim. Biophys. Acta.* 415:29–79.

39. Lash, J. 1995. Interaction of detergents with lipid vesicles. *Biochim. Biophys. Acta.* 1241:269–292.

40. Heerklotz, H. H., H. Binder, and H. Schmiedel. 1998. Excess enthalpies of mixing in phospholipid-additive membranes. *J. Phys. Chem.* 102:5363–5368.

41. Haydon, D. A., and J. Taylor. 1963. The stability and properties of bimolecular lipid leaflets in aqueous solutions. *J. Theor. Biol.* 4:281–296.

42. Kopecki, F. 1996. Micellization and other associations of amphiphilic antimicrobial quaternary ammonium salts in aqueous solutions. *Pharmazie.* 51:135–144.